

PCCP

Accepted Manuscript



This is an *Accepted Manuscript*, which has been through the Royal Society of Chemistry peer review process and has been accepted for publication.

Accepted Manuscripts are published online shortly after acceptance, before technical editing, formatting and proof reading. Using this free service, authors can make their results available to the community, in citable form, before we publish the edited article. We will replace this *Accepted Manuscript* with the edited and formatted *Advance Article* as soon as it is available.

You can find more information about *Accepted Manuscripts* in the [Information for Authors](#).

Please note that technical editing may introduce minor changes to the text and/or graphics, which may alter content. The journal's standard [Terms & Conditions](#) and the [Ethical guidelines](#) still apply. In no event shall the Royal Society of Chemistry be held responsible for any errors or omissions in this *Accepted Manuscript* or any consequences arising from the use of any information it contains.



PCCP

PAPER

From globule to crystal: a spectral study of poly(2-isopropyl-2-oxazoline) crystallization in hot water

Shengtong Sun^{*a,b} and Peiyi Wu^{*a}Received 00th January 20xx,
Accepted 00th January 20xx

DOI: 10.1039/x0xx00000x

www.rsc.org/

One easy strategy to comprehend the complex folding/crystallization behaviors of proteins is to study the self-assembly process of their synthetic polymeric analogues with similar properties owing to their simple structures and easy access to molecular design. Poly(2-isopropyl-2-oxazoline) (PIPOZ) is often regarded as an ideal pseudopeptide with similar two-step crystallization behavior to proteins, whose aqueous solution experiences a successive lower critical solution temperature (LCST)-type liquid-liquid phase separation upon heating and an irreversible crystallization when annealed above LCST for several hours. In this paper, by microscopic observations, IR and Raman spectroscopy in combination with 2D correlation analysis, we show that the second step of PIPOZ crystallization in hot water can be further divided into two apparent stages, i.e., nucleation and crystal growth, and perfect crystalline PIPOZ chains are found to only develop in the second stage. While all the groups exhibit changes in the initial nucleation, only methylene groups on the backbone participate in the crystal growth stage. During nucleation, a group motion transfer is found from side chain to the backbone, and the nucleation is assumed to be mainly driven by the cleavage of bridging C=O...D-O-D...O=C hydrogen bonds followed by chain arrangement due to the amide dipolar orientation. Nevertheless, during crystal growth, a further chain ordering process occurs resulting in the final formation of crystalline PIPOZ chains with partial *trans* conformation of backbones and alternative side chains on the two sides. The underlying crystallization mechanism of PIPOZ in hot water we present here may provide very useful information for understanding the crystallization of biomacromolecules in biological systems.

Introduction

The knowledge of the mechanism of protein folding/crystallization is crucial to comprehend many life phenomena.^{1, 2} However, the structure of protein is rather complex which largely restricts the understanding of the internal nature of such behavior. Therefore, owing to the facilely tailored chemical structures and functionalities, synthetic polymers with similar crystallization behavior provide an easy way to uncover the changes and interactions involved in the self-assembly process of biomolecules. Among them, poly(2-oxazoline)s, often regarded as polypeptide isomers, represent an important class of stimuli-responsive and crystallizable bioinspired polymers^{3, 4}, which have found many applications in biomaterials⁵⁻⁷, coatings⁸, composites^{9, 10}, etc. By adjusting its amphiphilicity such as side chain length¹¹, copolymerization¹²⁻¹⁴, or end group functionalization^{15, 16}, poly(2-oxazoline) in water can exhibit a lower critical solution

temperature (LCST)-type phase separation in a wide range of transition temperatures. Additionally, akin to protein crystallization, a few poly(2-oxazoline)s and their derivatives exhibit an irreversible crystallization process when annealing their solutions at a temperature higher than LCST for several hours^{10, 17-23}.

Poly(2-isopropyl-2-oxazoline) (PIPOZ) has an isomeric structure of poly(*N*-isopropylacrylamide) (PNIPAM)²⁴⁻²⁶, and shows also a similar LCST very close to the body temperature.²⁷ Thus, PIPOZ is often regarded as an ideal alternative to PNIPAM due to its nontoxicity and tunable LCST.^{28, 29} Nevertheless, unlike PNIPAM, PIPOZ chains crystallize irreversibly either in solid state³⁰ or in various solvents such as water^{17, 18}, organic solvents³¹ as well as organic/water mixtures³². Especially, upon prolonged heating above LCST, fiber-like PIPOZ crystals can evolve from a dense liquid aqueous phase. This process with the first formation of dense liquid droplets (or LCST-type coil-to-globule phase transition) prior to nucleation within the liquid intermediate is quite similar to the known two-step crystallization mechanism of proteins³³. Therefore, unravelling the crystallization mechanism of PIPOZ in water would be rather helpful to our understanding of the protein crystallization behavior.

Up to the present, several researches have been devoted to comprehending the crystallization process of PIPOZ in hot water. For instance, Demirel et al. made a structural investigation of crystalline PIPOZ nanofibers, and non-specific

^aState Key Laboratory of Molecular Engineering of Polymers, Collaborative Innovation Center of Polymers and Polymer Composite Materials, Department of Macromolecular Science and Laboratory for Advanced Materials, Fudan University, Shanghai 200433, China. E-mail: peiyiwu@fudan.edu.cn

^bState Key Laboratory of Chemical Engineering, East China University of Science and Technology, Meilong Road 130, Shanghai 200237, China. E-mail: shengtongsun@gmail.com

[†]Electronic Supplementary Information (ESI) available: time-variable IR spectra of PIPOZ during annealing between 120 and 340 min, sequential order determination details for 2DCOS. See DOI: 10.1039/x0xx00000x

interactions of side chains and amide $N^+=C-O^-$ dipole orientation were assumed to contribute to the chain ordering process of PIPOZ. Also, solvation of the polymer is supposed to be especially important in lowering the kinetic barriers in the crystallization.¹⁷ Later, despite a few reports on morphological studies^{18,20}, still no experimental evidence for such mechanism has been reported. Vibrational spectroscopy is very helpful to study conformational changes of polymeric systems owing to its high sensitivity to subtle variations. For example, Katsumoto et al. used IR spectroscopy to dissect the mechanism of the heat-induced phase separation of PIPOZ through LCST (the first step prior to nucleation).²² Unfortunately, no reliable IR spectra in their work for monitoring the second crystallization process were presented, and only molecular orbital calculations were carried out to predict the possible formation of mostly *all-trans* conformation of PIPOZ backbones. Experimental proof for the conformational changes during crystallization is still lacking, especially from the perspective of vibrational spectroscopy.

Herein, we show that the second crystallization process of PIPOZ in hot water can also be primely traced by IR spectroscopy, and perturbation correlation moving window (PCMW) and two-dimensional correlation spectroscopy (2DCOS) analyses were also used to extract more information from 1D IR spectra, as what we did to study the structural changes during the reversible phase transition processes of PIPOZ hydrogel³⁴ and aqueous solutions^{35, 36}. Microscopic observations and Raman spectroscopy also helped our analysis. For the first time, two apparent stages after liquid-liquid phase separation, i.e., nucleation and crystal growth, of PIPOZ crystallization in hot water were elucidated benefiting from the vibrational sensitivity to subtle group changes and a sequential order determination. The driving forces for PIPOZ nucleation were found to be the gradual cleavage of C=O related hydrogen bonds in side chains and subsequent amide dipolar orientation to favor an ordered chain arrangement.

Experimental

Materials

PIPOZ was prepared *via* cationic ring-opening polymerization of 2-isopropyl-2-oxazoline (Tokyo Chemical Industry Co. Ltd.) initiated with methyl tosylate, according to the literature³⁷. The number-average molecular weight (M_n) and polydispersity index ($PDI = M_w/M_n$) were determined by GPC measurements with monodisperse polystyrene as standard and THF as the eluent. For PIPOZ used in this paper, $M_n = 13,400 \text{ g}\cdot\text{mol}^{-1}$, and $PDI = 1.16$. Before IR and Raman measurements, PIPOZ was dissolved in deuterated water (D_2O) with a weight ratio of 10 wt% and the resultant solution was incubated at 4 °C for a week to ensure complete dissolution and deuteration.

Instruments and measurements

The sample of PIPOZ solution for IR measurements was prepared by sealing a proper amount of solution between two CaF_2 tablets. Then the liquid cell was heated to 55 °C at a rate of 2 °C/min and annealed at this temperature for 20 hours

(1200 min). Time-dependent IR spectra were collected on a Nicolet Nexus 6700 spectrometer with an interval of 10 min. A resolution of 4 cm^{-1} and 32 scans were applied for an acceptable signal-to-noise ratio. Raw spectra were baseline-corrected by the software Omnic, ver. 6.1a. The sample for Raman measurements is the same solution to IR but was sealed in a capillary. Raman spectra were recorded on a Renishaw inVia Reflex micro-Raman spectrometer with He/Ne laser excitation at 632.8 nm. Temperature was controlled at 55 °C by a temperature-controlled stage (Linkam, THMS-600). For optical microscopic observation, a drop of PIPOZ aqueous solution (10 wt%) was sealed between two glass plates and images were taken on a Leica light microscope at the same annealing temperature of 55 °C. High-resolution TEM image and electron diffraction of PIPOZ crystals were taken with a JEOL JEM 2011 at 200 kV. The sample for high-resolution TEM was prepared by evaporating a small drop of the sample solution on a carbon coated copper grid which was already annealed at 55 °C for 20 hours.

Investigation methods

Perturbation correlation moving window (PCMW). FT-IR spectra collected with an increment of 10 min during thermal annealing were used to perform PCMW analysis. Primary data processing was carried out with the method Morita provided and further correlation calculation was performed using the software 2D Shige, ver. 1.3 (© Shigeaki Morita, Kwansai-Gakuin University, Japan, 2004-2005). The final contour maps were plotted by Origin program, ver. 9.2, with warm colors (red and yellow) defined as positive intensities and cool colors (blue) as negative ones. An appropriate window size ($2m + 1 = 21$) was chosen to generate PCMW spectra with good quality.

2D correlation spectroscopy (2DCOS). FT-IR spectra chosen from PCMW analysis were used to perform 2D correlation analysis. 2D correlation analysis was carried out using the same software 2D Shige ver. 1.3 (© Shigeaki Morita, Kwansai-Gakuin University, Japan, 2004-2005), and was further plotted into the contour maps by Origin program, ver. 9.2. In the contour maps, warm colors (red and yellow) are defined as positive intensities, while cool colors (blue) as negative ones.

Results and discussion

Microscopic observation

PIPOZ is known to crystallize in hot water after an LCST-type liquid-liquid phase separation.^{17, 22} Thus, for comparison, it is necessary to observe visually the evolution of PIPOZ crystals upon prolonged heating at a temperature of 55 °C that we used for the following spectroscopic measurements. As shown in Fig. 1a, apparent morphological changes can be observed from the optical microscopic images at different time. First, plenty of droplets are visible at the beginning (60 min) which represent the dense liquid phases of PIPOZ after liquid-liquid phase separation³⁶. Within 180 min, the size of droplets only slightly grows while from 180 to 360 min, the droplets coalescence and fuse together along with coarse-graining

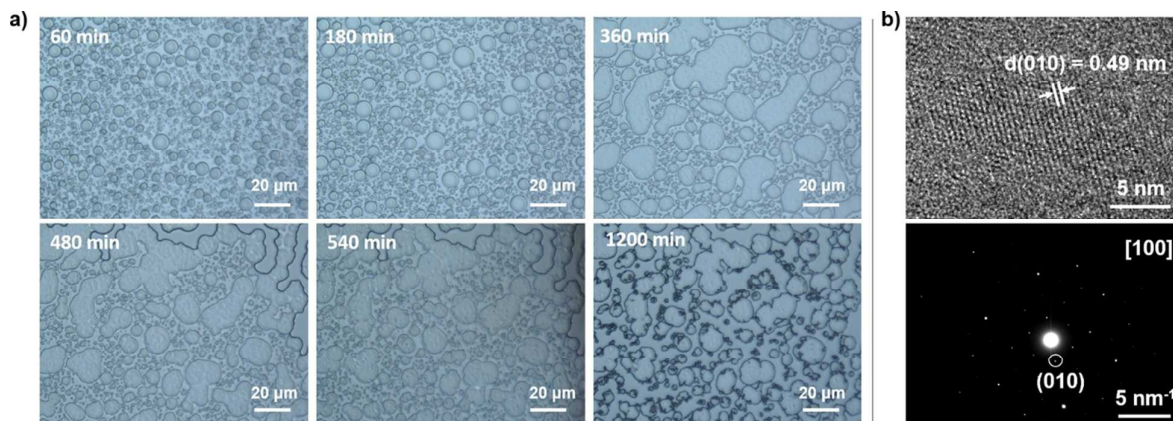


Fig. 1 (a) Optical micrographs of the evolution of PIPOZ crystals from its aqueous solution (10 wt%) at different time when annealed at 55 °C. (b) High-resolution TEM image and corresponding single-crystalline electron diffraction pattern of PIPOZ crystal viewed along the direction of [100]. The lattice spacing of 0.49 nm corresponds to the (010) face.

inside the droplets. The coarse-graining indicates the initial appearance of solid phases, and the period before that can be regarded as the first stage of PIPOZ crystallization, or nucleation. From 360 to 1200 min, the size of PIPOZ droplets does not change much while the solidification of the dense liquid phases is always proceeding which finally results in the formation of densified solid phases at 1200 min. This stage is assumed to be the growth of PIPOZ crystals. Therefore, the crystallization of PIPOZ in hot water can be roughly divided into two stages, i.e., nucleation and crystal growth. The nucleation stage seems to be finished within 360 min when annealed the aqueous solution of PIPOZ at 55 °C.

The single crystalline structure of PIPOZ evolving from its hot aqueous solution can be confirmed by high-resolution TEM and electron diffraction, as shown in Fig. 1b. The lattice spacing of 0.49 nm corresponds to the (010) face of PIPOZ crystals, which can also be observed in the electron diffraction pattern. As reported, the (010) direction is almost perpendicular to the ordered PIPOZ backbones, and thus 0.49 nm is actually the spacing between two PIPOZ chains.¹⁷

Conventional IR analysis

In a previous study by Katsumoto et al., ATR-IR spectroscopy failed to monitor the crystallization process of PIPOZ in hot water due to some instrumental limitations.²² Here, our method by sealing the PIPOZ aqueous solution between two CaF₂ tablets for transmission IR can solve this problem by effectively prohibiting the evaporation of solvents during measurement. The annealing temperature was chosen to be 55 °C, which is above the LCST of PIPOZ phase separation (~37 °C)³⁶, and also allows for the crystallization of PIPOZ chains within 20 hours as shown in microscopic observations. D₂O instead of H₂O was used as the solvent in order to eliminate the overlap of the δ(O-H) band of H₂O around 1640 cm⁻¹ with ν(C=O) bands as well as the broad ν(O-H) band of H₂O around 3300 cm⁻¹ with ν(C-H) bands of PIPOZ.^{26, 38} The deuterium

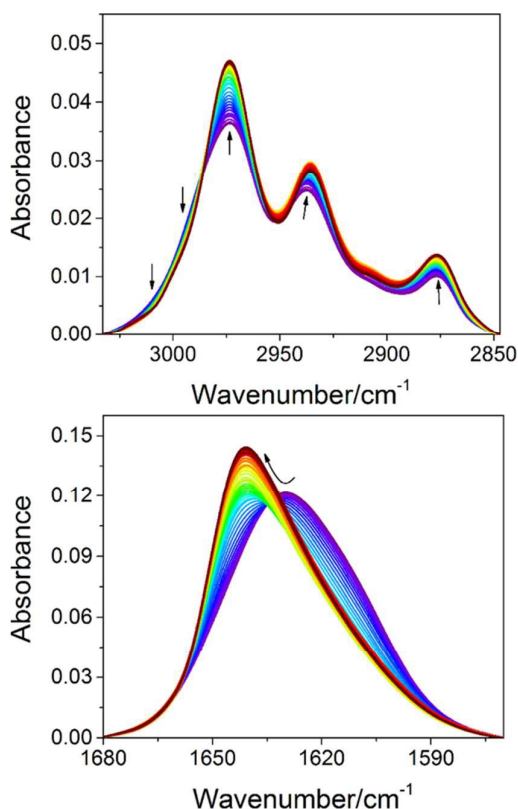


Fig. 2 Time-dependent FTIR spectra of PIPOZ in D₂O (10 wt%) annealed at 55 °C for 1200 min in the regions: 3030-2847 cm⁻¹ and 1680-1570 cm⁻¹. For clarity, only a 20 min interval is shown. The arrows indicate the directions of spectral variations.

isotope effect was reported to cause no obvious changes of the phase behavior of water-soluble polymers.^{38, 39}

Here, we mainly focus on two spectral regions of PIPOZ: C-H stretching region (3030-2847 cm⁻¹), and C=O stretching region (1680-1570 cm⁻¹) – with them, we can trace nearly all

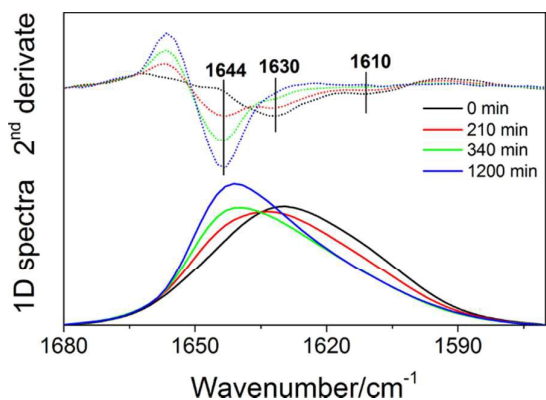


Fig. 3 FTIR spectra and corresponding second derivative curves of C=O stretching band of PIPOZ during annealing at 0, 210, 340, and 1200 min.

group motions during crystallization. As shown in Fig. 2, during annealing, all the groups show some changes, as indicated by the arrows. For instance, the asymmetric and symmetric C-H stretching bands of methyl groups ($\nu_{\text{as}}(\text{CH}_3)$ and $\nu_{\text{s}}(\text{CH}_3)$) at 2974 cm^{-1} and 2876 cm^{-1} respectively show continuous spectral

intensity increasing during annealing while the two shoulder bands around 3010 and 2991 cm^{-1} have the spectral intensities decreased. The latter two bands can be assigned to $\nu_{\text{as}}(\text{CH}_3)$ in $\text{CH}_3\cdots\text{O}=\text{C}$ hydrogen bonds, which can also be observed in the dehydration process of PIPOZ aqueous solutions³⁶. This assignment is reasonable because the formation of $\text{C-H}\cdots\text{O}=\text{C}$ hydrogen bonds would shorten the length of C-H bond leading to much higher wavenumbers⁴⁰⁻⁴². It is noted that the presence of $\text{C-H}\cdots\text{O}=\text{C}$ hydrogen bonds was also found in the poly(L-lactide) and poly(3-hydroxybutyrate) systems⁴³⁻⁴⁵. The intensity decrease of these two bands during PIPOZ crystallization is due to the breakage of $\text{CH}_3\cdots\text{O}=\text{C}$ hydrogen bonds, which are unfavorable for the ordered self-assembly of PIPOZ chains. Obviously, the amount increase of dehydrated methyl groups (2974 cm^{-1}) is at the expense of consuming $\text{CH}_3\cdots\text{O}=\text{C}$ hydrogen bonds, which frees methyl groups for the ordered packing during crystallization.

It is also noted that both the frequencies of $\nu_{\text{as}}(\text{CH}_3)$ at 2974 cm^{-1} and $\nu_{\text{s}}(\text{CH}_3)$ at 2876 cm^{-1} do not change during the whole annealing process, indicating that the majority of methyl groups in side chains remain at the dehydrated state before and after crystallization. However, $\nu_{\text{as}}(\text{CH}_2)$ around 2937 cm^{-1} shows a slight frequency shift to lower wavenumbers.

This reveals that the backbone of PIPOZ exhibits a further dehydration process (although minor) during annealing at the temperature above LCST. It is reasonable since water molecules are mainly existing in the form of $\text{C}=\text{O}\cdots\text{D}-\text{O}-\text{D}\cdots\text{O}=\text{C}$ hydrogen bonding bridges in the collapsed PIPOZ chains after phase separation³⁶, and thus the methylene groups on the backbone are still slightly hydrated due to the existence of water molecules around amide groups which are adjacent to them. During crystallization, loss of water molecules occurs, which inevitably causes the further dehydration of methylene groups resulting in PIPOZ crystals free of water.

C=O groups show a binary spectral variation during annealing, as shown in Fig. 2. For clarity, we plotted several IR spectra and their second derivative curves in Fig. 3. Second derivative curves apparently indicate the existence of three main peaks at 1644 , 1630 , and 1610 cm^{-1} , respectively. Upon annealing, the peaks at 1630 and 1610 cm^{-1} are gradually disappearing while the peak at 1644 cm^{-1} emerges. The former two peaks are assigned to the stretching bands of C=O in $\text{C}=\text{O}\cdots\text{D}-\text{O}-\text{D}\cdots\text{O}=\text{C}$ hydrogen bonds and $\text{C}=\text{O}\cdots\text{D}_2\text{O}$ hydrogen bonds, respectively, while the latter one arises from ordered C=O in crystalline PIPOZ chains.^{35,36,46} The spectral changes of C=O stretching bands reveal that the crystallization of PIPOZ in hot water is accompanied by the cleavage of C=O related hydrogen bonds and the formation of ordered carbonyl groups.

To quantitatively examine the spectral changes of methyl, methylene and carbonyl groups, the spectral intensity change of $\nu_{\text{as}}(\text{CH}_3)$ at 2974 cm^{-1} , the frequency shift of $\nu_{\text{as}}(\text{CH}_2)$, and the frequency shift of $\nu(\text{C}=\text{O})$ as a function of time were plotted in Fig. 4. The Boltzmann fitting method which is frequently used for fitting sigmoid changes in phase transition systems⁴⁷⁻⁴⁹ was used to fit the data points. Interestingly, all the points for the spectral intensity change of $\nu_{\text{as}}(\text{CH}_3)$ and the frequency change of $\nu(\text{C}=\text{O})$ can be fitted well with a long trailing after ca. 400 min. However, the frequency shift of $\nu_{\text{as}}(\text{CH}_2)$ deviates a lot from the Boltzmann fitted line (dashed line in Fig. 4b) after ca. 300 min. It is presumed that the dehydration of methylene groups can be divided into two distinct stages, which are ascribed to nucleation and crystal growth, respectively, on the basis of the above microscopic observations. The comparison of spectral changes between CH_3 , CH_2 and C=O groups strongly indicates us that all of them would participate in the nucleation process with sigmoid variations while only methylene groups take part in the crystal growth process. This finding is important for unravelling the mechanism of PIPOZ crystallization in hot water.

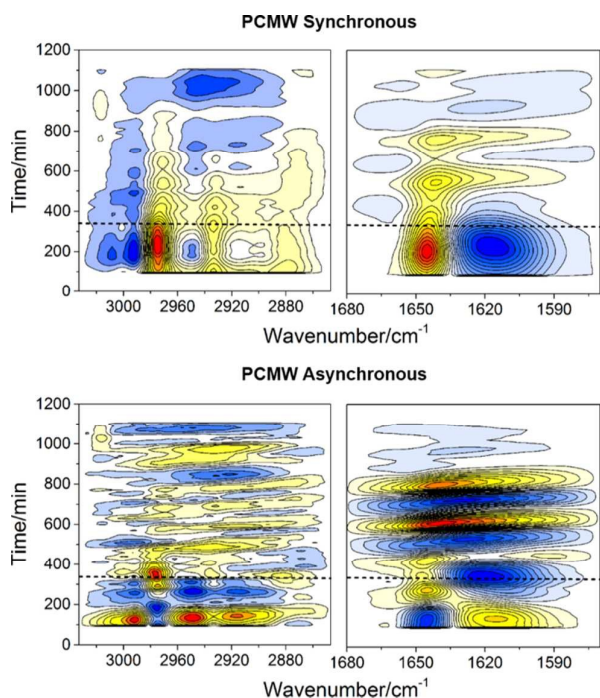


Fig. 5 PCMW synchronous and asynchronous spectra of PIPOZ in D₂O (10 wt%) during annealing for 1200 min. Wherein, warm colors (red and yellow) are defined as positive intensities, while cool colors (blue) as negative ones. The dashed line represents the time point at 340 min separating nucleation and crystal growth stages.

Perturbation correlation moving window

From 1D IR spectral analysis, it is difficult to determine the time ranges for the two stages of PIPOZ crystallization due to the subtle spectral changes and easily disturbed spectral curves during IR collection at such a high temperature and within such a long period. Therefore, PCMW was employed to assist our analysis. PCMW is a newly developed technique, whose basic principles can date back to conventional moving window proposed by Thomas et al.⁵⁰, and later in 2006 Morita et al.⁵¹ improved this technique to much wider applicability through introducing the perturbation variable into correlation equation. Except for its original ability in determining transition points as conventional moving window did, PCMW

can additionally monitor complicated spectral variations along the perturbation direction.

Fig. 5 presents PCMW synchronous and asynchronous spectra of PIPOZ aqueous solution during annealing at 55 °C for 1200 min. It is noted that although not easy to discern in conventional IR, the peak variations of the two bands at 3010 and 2991 cm⁻¹ arising from CH₃...O=C hydrogen bonds are quite recognizable in PCMW spectra. PCMW synchronous spectra are very helpful to find transition points while asynchronous spectra provide the information about transition ranges. The spectral variations along time perturbation can be monitored combining the signs of synchronous and asynchronous spectra by the following rules: in the case of perturbation increment, positive synchronous correlation represents spectral intensity increasing, while negative one represents decreasing; positive asynchronous correlation can be observed for a convex spectral intensity variation while negative one can be observed for a concave variation.⁵¹ In the case of PIPOZ crystallization, two stages can also be discerned by PCMW. The nucleation stage exhibits obvious sigmoid changes with the transition time at ~200 min and the transition range from 120 to 340 min. We plotted the time-variable IR spectra of the nucleation stage between 120 to 340 min in Fig. S1. Interestingly, for both $\nu_{as}(\text{CH}_3)$ and $\nu(\text{C}=\text{O})$, isosbestic points can be observed at 2986 and 1635 cm⁻¹, respectively, indicating the direct transformation of methyl groups from CH₃...O=C hydrogen bonds to dehydrated CH₃ and the direct transformation of carbonyl groups from hydrogen bonded amides to ordered ones free of water.⁵² As indicated by the dashed line in Fig. 5, 340 min can be regarded as the segmental time point, after which crystal growth dominates the whole process. Since the spectral variations during the crystal growth stage are rather small and easily disturbed by the background, no regular changes can be recognized in this stage. This is understandable that from conventional IR analysis we know only changes of methylene groups are dominating in the crystal growth stage, which is assumed to be the backbone torsion and arrangement to adapt to the final structure of PIPOZ crystals.

As we stated before, PCMW can serve as an important basis for the segmental mode of 2DCOS.⁵³ In this paper, only the spectra in the nucleation stage will be analyzed by 2DCOS. It should be noted that 2DCOS analysis of a spectral region

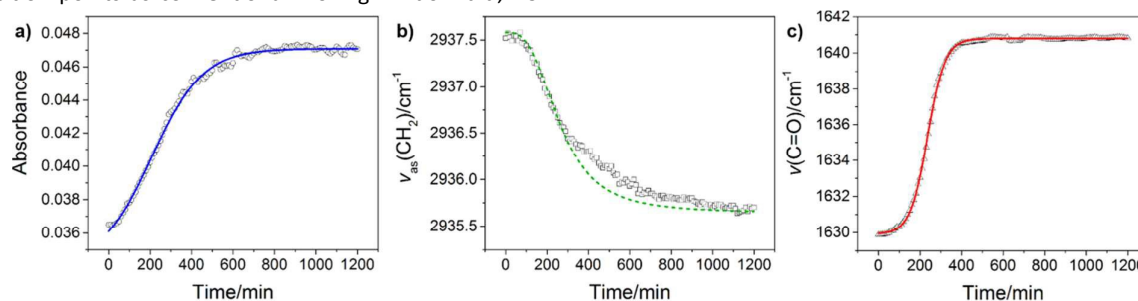


Fig. 4 (a) Spectral intensity change of $\nu_{as}(\text{CH}_3)$ at 2974 cm⁻¹, (b) frequency shift of $\nu_{as}(\text{CH}_2)$, and (c) frequency shift of $\nu(\text{C}=\text{O})$ as a function of time. The solid and dashed lines represent the fitted curves according to the Boltzmann fitting method.

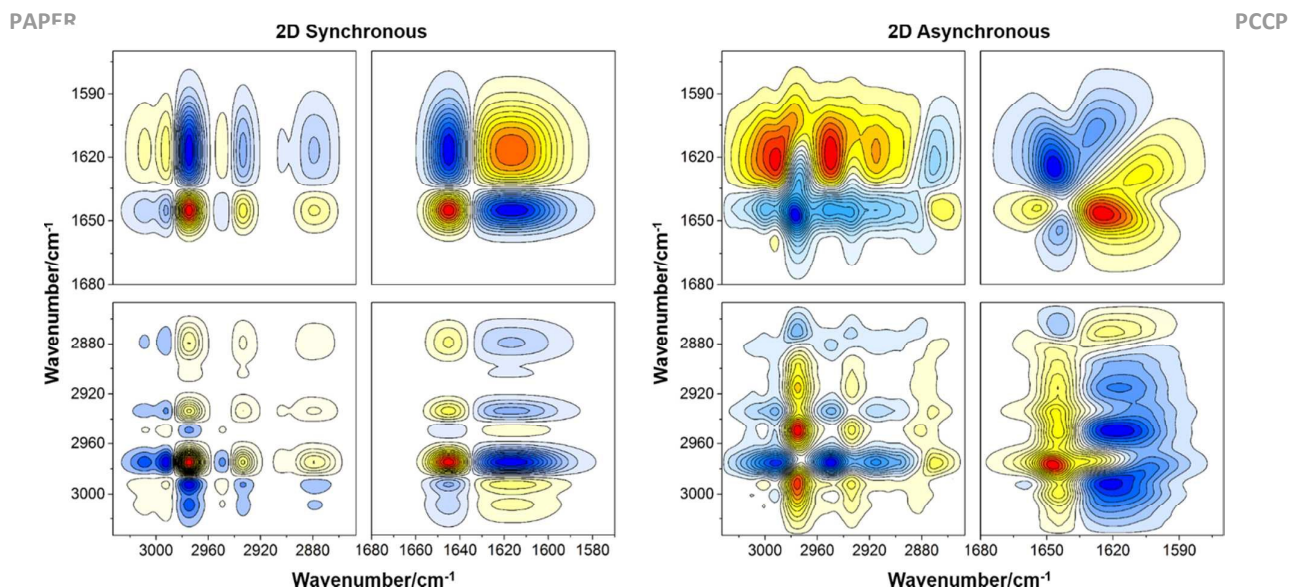


Fig. 6 2DCOS synchronous and asynchronous spectra of PIPOZ nucleation in D₂O (10 wt%) during annealing at 55 °C between 120 and 340 min. Wherein, warm colors (red and yellow) are defined as positive intensities, while cool colors (blue) as negative ones.

with much noise like the crystal growth stage in this paper is very dangerous because 2DCOS will significantly magnify the influence of noise, which of course cannot give reliable results.

2D correlation analysis

2DCOS is a mathematical method whose basic principles were first proposed by Noda in 1986.⁵⁴ Up to the present, 2DCOS has been widely used to study spectral variations of different chemical species under various external perturbations (e.g. temperature, pressure, concentration, time, electromagnetic, etc).⁵⁵ Due to the different response of different species to external variable, additional useful information about molecular motions or conformational changes can be extracted which cannot be obtained straight from conventional 1D spectra.

On the basis of the nucleation time range obtained from PCMW, we chose all the spectra between 120 and 340 min to perform 2DCOS analysis, as shown in Fig. 6. 2D synchronous spectra reflect simultaneous changes between two given wavenumbers. For instance, the peaks at 2991 and 2974 cm⁻¹ have negative cross-peaks, indicating that they have an opposite response of spectral intensities to the time perturbation, which, in conventional IR, show a binary spectral variation. 2D synchronous spectrum can be regarded as a two-dimensional depiction of spectral variations in raw spectra.

2D asynchronous spectra can significantly enhance the spectral resolution. In Fig. 6, many subtle bands hidden in 1D spectra can be identified, such as the bands at 2881 and 2872 cm⁻¹ contributing from $\nu_s(\text{CH}_3)$ (ordered) and $\nu_s(\text{CH}_3)$ (disordered), respectively. Four splitting peaks of $\nu(\text{C}=\text{O})$ can also be discerned at 1655, 1644, 1630, and 1610 cm⁻¹, respectively, corresponding to free C=O, ordered C=O at the crystalline state, C=O...D-O-D...O=C hydrogen bonds, and C=O...D₂O hydrogen bonds, respectively. For the convenience of discussion, all the bands found in the asynchronous spectra and their tentative assignments have been presented in Table 1. Note that the peak at 2951 cm⁻¹ in Fig. 6 is actually a trough

and cannot be assigned to any groups, which will not be discussed in this paper.

Table 1 Tentative band assignments of PIPOZ during nucleation process according to 2DCOS results^{22, 34-36, 46}

Wavenumber/cm ⁻¹	Assignment
3010	$\nu_{\text{as}}(\text{CH}_3)(\text{CH}_3\cdots\text{O}=\text{C})$
2991	$\nu_{\text{as}}(\text{CH}_3)$ (dehydrated)
2974	$\nu_{\text{as}}(\text{CH}_3)$ (dehydrated)
2937	$\nu_{\text{as}}(\text{CH}_2)$
2912	$\nu(\text{CH})$
2881	$\nu_s(\text{CH}_3)$ (ordered)
2872	$\nu_s(\text{CH}_3)$ (disordered)
1655	$\nu(\text{C}=\text{O})$ (free)
1644	$\nu(\text{C}=\text{O})$ (ordered)
1630	$\nu(\text{C}=\text{O})(\text{C}=\text{O}\cdots\text{D}-\text{O}-\text{D}\cdots\text{O}=\text{C})$
1610	$\nu(\text{C}=\text{O})(\text{C}=\text{O}\cdots\text{D}_2\text{O})$

Except for enhancing spectral resolution, 2DCOS can also discern the specific order taking place under external perturbation. The judging rule can be summarized as Noda's rule – that is, if the cross-peaks (ν_1 , ν_2 , and assume $\nu_1 > \nu_2$) in synchronous and asynchronous spectra have the same sign, the change at ν_1 occurs prior to that of ν_2 , and vice versa. As space is limited, the determination details of sequential orders have been presented in ESI, and only the final specific order for the nucleation process of PIPOZ in hot water is given as follows (\rightarrow means prior to or earlier than): 3010 cm⁻¹ \rightarrow 2991 cm⁻¹ \rightarrow 2912 cm⁻¹ \rightarrow 1655 cm⁻¹ \rightarrow 2872 cm⁻¹ \rightarrow 1644 cm⁻¹ \rightarrow 1610 cm⁻¹ \rightarrow 2881 cm⁻¹ \rightarrow 2974 cm⁻¹ \rightarrow 2937 cm⁻¹ \rightarrow 1630 cm⁻¹, or $\nu_{\text{as}}(\text{CH}_3)(\text{CH}_3\cdots\text{O}=\text{C})$ (3010 cm⁻¹) \rightarrow $\nu_{\text{as}}(\text{CH}_3)(\text{CH}_3\cdots\text{O}=\text{C})$ (2991 cm⁻¹) \rightarrow $\nu(\text{CH})$ \rightarrow $\nu(\text{C}=\text{O})$ (free) \rightarrow $\nu_s(\text{CH}_3)$ (disordered) \rightarrow $\nu(\text{C}=\text{O})$ (ordered) \rightarrow $\nu(\text{C}=\text{O})(\text{C}=\text{O}\cdots\text{D}_2\text{O})$ \rightarrow $\nu_s(\text{CH}_3)$ (ordered) \rightarrow $\nu_{\text{as}}(\text{CH}_3)$ (dehydrated) \rightarrow $\nu_{\text{as}}(\text{CH}_2)$ \rightarrow $\nu(\text{C}=\text{O})(\text{C}=\text{O}\cdots\text{D}-\text{O}-\text{D}\cdots\text{O}=\text{C})$.

Without considering different vibrational modes, this sequence order can be further summarized as: $\text{CH}_3\cdots\text{O}=\text{C} \rightarrow \text{CH} \rightarrow \text{C}=\text{O} \rightarrow \text{CH}_2$. Interestingly, the sequence just represents a group motion transfer from side chain to backbone indicating that the crystallization of PIPOZ starts from the side chain movement followed by the backbone rearrangement. The driving forces of PIPOZ nucleation in hot water are the cleavage of two kinds of hydrogen bonds, i.e., $\text{CH}_3\cdots\text{O}=\text{C}$ hydrogen bonds and $\text{C}=\text{O}\cdots\text{water}$ hydrogen bonds. As shown in conventional IR analysis, the cleavage of these two kinds of hydrogen bonds both exhibits isosbestic points by direct transformation to free methyl and amide groups. In other words, the bridging interactions including $\text{CH}_3\cdots\text{O}=\text{C}$ hydrogen bonds and $\text{C}=\text{O}\cdots\text{D}-\text{O}-\text{D}\cdots\text{O}=\text{C}$ hydrogen bonds formed during the liquid-liquid phase separation will be destroyed first by chain reordering and further loss of water molecules in the nucleation stage of PIPOZ. Since $\text{CH}_3\cdots\text{O}=\text{C}$ hydrogen bonds are not largely formed judged from raw spectra, the driving force for PIPOZ nucleation will be mainly the cleavage of $\text{C}=\text{O}\cdots\text{D}-\text{O}-\text{D}\cdots\text{O}=\text{C}$ hydrogen bonds. Induced by the side chain movement, the backbone of PIPOZ will distort to adapt to more closely packed side chains, while the driving force for this step should be the amide dipolar orientation as reported previously¹⁷.

Determined from optical micrographs, nucleation of PIPOZ does not produce perfect crystalline chains, which only develop in the crystal growth stage. Conventional IR analysis showed us that only methylene groups will participate in the second stage. It is speculated that the crystal growth stage is just the further chain ordering process of PIPOZ backbones with conformational changes resulting in the final formation of ordered crystalline PIPOZ chains. While IR and 2D analysis cannot give more information about the conformational changes of PIPOZ chains, we utilized Raman spectroscopy to study this process.

Raman spectroscopy

For comparison, we measured the Raman spectra of PIPOZ aqueous solution in D_2O at 25 °C and 55 °C with different annealing time, respectively, as presented in Fig. 7a. The spectrum of PIPOZ aqueous solution at 25 °C corresponds to the hydrated state below LCST while that at 55 °C corresponds to the dehydrated state above LCST. The annealing time of 240 and 840 min falls into the nucleation stage and crystal growth stage respectively, which can

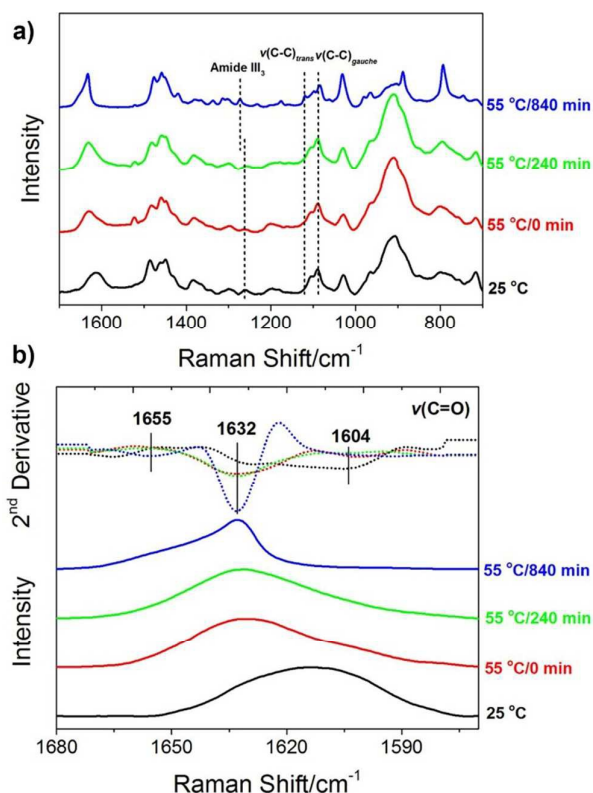


Fig. 7 a) Raman spectra of PIPOZ in D_2O (10 wt%) at 25 °C and 55 °C with annealing time of 0, 240, and 840 min, respectively. b) Stacked Raman spectra of $\nu(\text{C}=\text{O})$ region and corresponding second derivative curves.

be used to make clear spectral comparison between these two stages.

$\nu(\text{C}=\text{O})$ bands in Raman are very similar to the bands found in IR, despite minor frequency differences, as shown in Fig. 7b. Upon heating, $\nu(\text{C}=\text{O})$ shifts to higher wavenumbers indicating the dehydration process, which was also observed in our previous paper³⁶. Along with nucleation time, the shoulder peak at 1604 cm^{-1} corresponding to hydrogen bonded $\text{C}=\text{O}$ disappears, and a new peak at 1655 cm^{-1} emerges at the crystal growth stage, which can be ascribed to free $\text{C}=\text{O}$. Obviously, Raman is more sensitive to detect free $\text{C}=\text{O}$ than IR. In all, $\nu(\text{C}=\text{O})$ variations accord well with the gradual cleavage of hydrogen bonds during chain reordering.

Amide III₃ is also an indicator to show the disorder-to-order changes.⁵⁶ In the case of PIPOZ, the amide III₃ band shifts drastically from 1263 cm⁻¹ for a disordered state to 1273 cm⁻¹ for a crystalline state upon annealing for 840 min, indicating that the motion of amide groups plays an important role in the crystallization process, which, in the case of PIPOZ crystallization, should be the amide dipolar orientation. More importantly, Raman is known to be very sensitive to C-C skeleton conformational changes⁵⁷⁻⁵⁹. By comparing the peak intensities of C-C stretching band at ~1080 and ~1124 cm⁻¹ corresponding to *gauche* and *trans* conformations respectively, conformational order can be determined for alkyl chains⁶⁰⁻⁶². For PIPOZ aqueous solution, both the hydrated state at 25 °C and the nucleation stage at 55 °C annealed for 0 and 240 min do not show any information about the *trans* conformation of PIPOZ backbones. Nevertheless, the crystal growth stage of PIPOZ in hot water annealed for 840 min exhibits a shoulder peak at 1121 cm⁻¹, indicating the partial transformation of methylene groups from *gauche* to *trans*. However, an *all-trans* conformation of crystalline PIPOZ chains revealed by a previous molecular orbital calculation²² is not possible. Indeed, the periodicity of PIPOZ in the crystalline state was measured to be only 6.4 Å³⁰, while for the *all-trans* conformation the value is 7.6 Å. Therefore, most crystallized PIPOZ backbones are still a little distorted with a *gauche* conformation and alternative side chains are distributed on the two sides.

Above all, we proposed a mechanism to depict the whole process of PIPOZ crystallization in hot water at the molecular level, as illustrated in Fig. 8. Two stages, nucleation and crystal growth, can be distinguished. During nucleation, there exists a group motion transfer from side chain to the backbone driven by the cleavage of C=O related hydrogen bonds (C=O...D-O-D...O=C, C=O...D₂O, and CH₃...O=C hydrogen bonds) with water molecules expelled out of the polymer network (step 1). This is then followed by the chain arrangement due to the amide dipolar orientation (step 2). During

the crystal growth stage, a further chain ordering process occurs resulting in the final formation of crystalline PIPOZ chains with partial *trans* conformation of backbones and alternative side chains on the two sides (step 3).

Conclusions

In this paper, the crystallization mechanism of PIPOZ upon prolonged annealing above LCST was investigated by IR/Raman spectroscopy and microscopic observations. Following liquid-liquid phase separation through LCST, two apparent crystallization stages, nucleation and crystal growth, are distinguished for PIPOZ crystallization while crystalline solid phases develop only in the second stage. IR spectral analysis reveals that the cleavage of C=O related hydrogen bonds (C=O...D-O-D...O=C, C=O...D₂O, and CH₃...O=C hydrogen bonds), the further dehydration of PIPOZ backbones, and chain arrangement of side chains occur in the nucleation stage. However, only methylene groups participate in the crystal growth stage, i.e., the chains ordering process to form crystalline PIPOZ chains. PCMW helps with discerning these two stages at the segmental time point of 340 min, and the nucleation stage shows mostly sigmoid spectral changes with the transition time at ~200 min and the transition range from 120 to 340 min. 2DCOS analysis of the nucleation stage reveals a group motion transfer from side chain to the backbone, and the nucleation of PIPOZ is assumed to be mainly driven by the cleavage of bridging C=O...D-O-D...O=C hydrogen bonds followed by amide dipolar orientation. Raman spectroscopy was finally employed to elucidate the conformational changes in the crystal growth stage, in which perfect crystalline chains are formed with partial *trans* conformation of backbones and alternative side chains on the two sides. Since PIPOZ

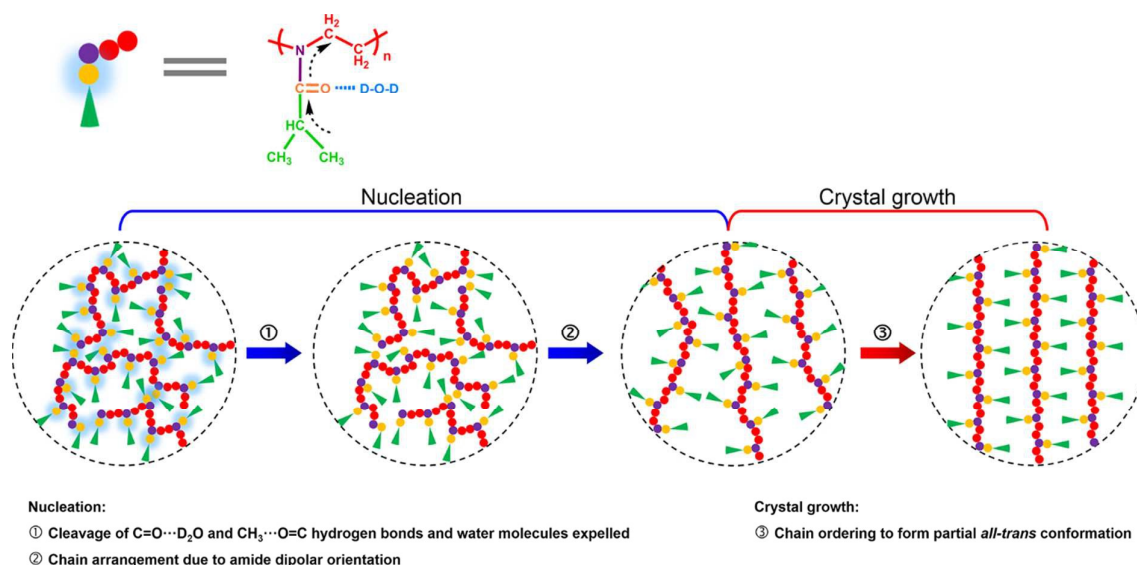


Fig. 8 Schematic illustration of PIPOZ crystallization starting from a globule upon prolonged annealing in hot water. The colored balls, triangles, and halos represent different atoms, groups, and hydrogen bonds, as illustrated on the top.

crystallization shares very similar two-step mechanism to proteins (liquid-liquid phase separation and subsequent nucleation/crystallization), our findings in this paper could be very helpful to understand various crystallization phenomena of biomacromolecules in biological systems.

Acknowledgements

We gratefully acknowledge the financial support from the National Science Foundation of China (NSFC) (nos 21274030, 51473038).

Notes and references

- S. D. Durbin and G. Feher, *Annu. Rev. Phys. Chem.*, 1996, **47**, 171-204.
- C. M. Dobson, *Nature*, 2003, **426**, 884-890.
- R. Hoogenboom, *Angew. Chem. Int. Ed.*, 2009, **48**, 7978-7994.
- R. Hoogenboom and H. Schlaad, *Polymers*, 2011, **3**, 467-488.
- O. Sedlacek, B. D. Monnery, S. K. Filippov, R. Hoogenboom and M. Hruby, *Macromol. Rapid Commun.*, 2012, **33**, 1648-1662.
- N. Adams and U. S. Schubert, *Adv. Drug Deliv. Rev.*, 2007, **59**, 1504-1520.
- M. Hartlieb, K. Kempe and U. S. Schubert, *J. Mater. Chem. B*, 2015, **3**, 526-538.
- L. Tauhardt, K. Kempe, M. Gottschaldt and U. S. Schubert, *Chem. Soc. Rev.*, 2013, **42**, 7998-8011.
- T. Ogoshi and Y. Chujo, *Polymer*, 2006, **47**, 4036-4041.
- N. Morimoto, R. Obeid, S. Yamane, F. M. Winnik and K. Akiyoshi, *Soft Matter*, 2009, **5**, 1597-1600.
- V. de la Rosa, *J. Mater. Sci.: Mater. Med.*, 2014, **25**, 1211-1225.
- R. Hoogenboom, H. M. L. Thijs, M. J. H. C. Jochems, B. M. van Lankvelt, M. W. M. Fijten and U. S. Schubert, *Chem. Commun.*, 2008, 5758-5760.
- J.-S. Park and K. Kataoka, *Macromolecules*, 2006, **39**, 6622-6630.
- J.-S. Park and K. Kataoka, *Macromolecules*, 2007, **40**, 3599-3609.
- S. Huber, N. Hutter and R. Jordan, *Colloid. Polym. Sci.*, 2008, **286**, 1653-1661.
- J.-S. Park, Y. Akiyama, F. M. Winnik and K. Kataoka, *Macromolecules*, 2004, **37**, 6786-6792.
- A. L. Demirel, M. Meyer and H. Schlaad, *Angew. Chem. Int. Ed.*, 2007, **46**, 8622-8624.
- M. Meyer, M. Antonietti and H. Schlaad, *Soft Matter*, 2007, **3**, 430-431.
- R. Obeid, F. Tanaka and F. M. Winnik, *Macromolecules*, 2009, **42**, 5818-5828.
- C. Diehl, P. Černoch, I. Zenke, H. Runge, R. Pitschke, J. Hartmann, B. Tiersch and H. Schlaad, *Soft Matter*, 2010, **6**, 3784-3788.
- P. T. Guner, A. Miko, F. F. Schweinberger and A. L. Demirel, *Polym. Chem.*, 2012, **3**, 322-324.
- Y. Katsumoto, A. Tsuchiizu, X. Qiu and F. M. Winnik, *Macromolecules*, 2012, **45**, 3531-3541.
- C. Legros, M.-C. De Pauw-Gillet, K. C. Tam, D. Taton and S. Lecommandoux, *Soft Matter*, 2015, **11**, 3354-3359.
- Y. Ono and T. Shikata, *J. Am. Chem. Soc.*, 2006, **128**, 10030-10031.
- B. Sun, Y. Lin, P. Wu and H. W. Siesler, *Macromolecules*, 2008, **41**, 1512-1520.
- S. Sun and P. Wu, *Macromolecules*, 2010, **43**, 9501-9510.
- H. Uyama and S. Kobayashi, *Chem. Lett.*, 1992, **21**, 1643-1646.
- J. Zhao, R. Hoogenboom, G. Van Assche and B. Van Mele, *Macromolecules*, 2010, **43**, 6853-6860.
- C. Diab, Y. Akiyama, K. Kataoka and F. M. Winnik, *Macromolecules*, 2004, **37**, 2556-2562.
- M. Litt, F. Rahl and L. G. Roldan, *J. Polym. Sci., Part A-2: Polym. Phys.*, 1969, **7**, 463-473.
- C. Legros, M.-C. De Pauw-Gillet, K. C. Tam, D. Taton and S. Lecommandoux, *Soft Matter*, 2015, **11**, 3354-3359.
- C. Diehl, I. Dambowsky, R. Hoogenboom and H. Schlaad, *Macromol. Rapid Commun.*, 2011, **32**, 1753-1758.
- P. R. t. Wolde and D. Frenkel, *Science*, 1997, **277**, 1975-1978.
- T. Li, H. Tang and P. Wu, *Soft Matter*, 2015, **11**, 1911-1918.
- T. Li, H. Tang and P. Wu, *Soft Matter*, 2015, **11**, 3046-3055.
- T. Li, H. Tang and P. Wu, *Langmuir*, 2015, **31**, 6870-6878.
- R. Obeid, E. Maltseva, A. F. Thünemann, F. Tanaka and F. M. Winnik, *Macromolecules*, 2009, **42**, 2204-2214.
- S. Sun and P. Wu, *Macromolecules*, 2013, **46**, 236-246.
- X. Wang and C. Wu, *Macromolecules*, 1999, **32**, 4299-4301.
- P. Hobza and Z. Havlas, *Chem. Rev.*, 2000, **100**, 4253-4264.
- T. Harada, H. Yoshida, K. Ohno and H. Matsuura, *Chem. Phys. Lett.*, 2002, **362**, 453-460.
- H. Matsuura, H. Yoshida, M. Hieda, S.-y. Yamanaka, T. Harada, K. Shin-ya and K. Ohno, *J. Am. Chem. Soc.*, 2003, **125**, 13910-13911.
- J. Zhang, H. Sato, I. Noda and Y. Ozaki, *Macromolecules*, 2005, **38**, 4274-4281.
- J. Zhang, H. Sato, H. Tsuji, I. Noda and Y. Ozaki, *J. Mol. Struct.*, 2005, **735-736**, 249-257.
- H. Sato, R. Murakami, A. Padermshoke, F. Hirose, K. Senda, I. Noda and Y. Ozaki, *Macromolecules*, 2004, **37**, 7203-7213.
- E. F. J. Rettler, H. M. L. Lambermont-Thijs, J. M. Kranenburg, R. Hoogenboom, M. V. Unger, H. W. Siesler and U. S. Schubert, *J. Mater. Chem.*, 2011, **21**, 17331-17337.
- S. Sun, H. Tang, P. Wu and X. Wan, *Phys. Chem. Chem. Phys.*, 2009, **11**, 9861-9870.
- S. Sun, J. Hu, H. Tang and P. Wu, *J. Phys. Chem. B*, 2010, **114**, 9761-9770.
- S. Sun and P. Wu, *Soft Matter*, 2011, **7**, 6451-6456.
- M. Thomas and H. H. Richardson, *Vib. Spectrosc.*, 2000, **24**, 137-146.
- S. Morita, H. Shinzawa, I. Noda and Y. Ozaki, *Appl. Spectrosc.*, 2006, **60**, 398-406.
- B. S. Berlett, R. L. Levine and E. R. Stadtman, *Anal. Biochem.*, 2000, **287**, 329-333.
- M. Wang, S. Sun and P. Wu, *Appl. Spectrosc.*, 2010, **64**, 1396-1406.
- I. Noda, *Bull. Am. Phys. Soc.*, 1986, **31**, 520.

PAPER

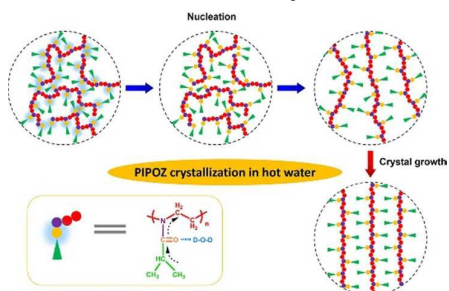
PCCP

55. I. Noda and Y. Ozaki, *Two-Dimensional Correlation Spectroscopy: Applications in Vibrational and Optical Spectroscopy*, Wiley, Chichester, 2004.
56. S. A. Asher, A. V. Mikhonin and S. Bykov, *J. Am. Chem. Soc.*, 2004, **126**, 8433-8440.
57. M. Pigeon, R. E. Prud'homme and M. Pérolet, *Macromolecules*, 1991, **24**, 5687-5694.
58. J. L. Koenig and A. C. Angood, *J. Polym. Sci., Part A-2: Polym. Phys.*, 1970, **8**, 1787-1796.
59. B. H. Stuart, *Vib. Spectrosc.*, 1996, **10**, 79-87.
60. R. J. Meier, *Polymer*, 2002, **43**, 517-522.
61. C. J. Orendorff, M. W. Ducey and J. E. Pemberton, *J. Phys. Chem. A*, 2002, **106**, 6991-6998.
62. H. Tang, S. Sun, J. Wu, P. Wu and X. Wan, *Polymer*, 2010, **51**, 5482-5489.

PCCP

PAPER

Table of Contents Entry



Two stages, nucleation and crystal growth, were distinguished by two-dimensional correlation infrared spectroscopy in the crystallization of poly(2-isopropyl-2-oxazoline) in hot water starting from globules.